Thermophysical Analysis of SU8-Modified Microstructures Created by Visible Light Lithography

DANIEL RODRIGUEZ PONCE,[1] KAREN LOZANO,[1] THOMAS EUBANKS,[2] AHMAD HARB,[1] DOMINGO FERRER,[3] YUANKUN LIN[4]

[1]Department of Mechanical Engineering, University of Texas-Pan American, Edinburg, Texas 78541

[2]Department of Biology, University of Texas-Pan American, Edinburg, Texas 78541

[3]Microelectronics Research Center, University of Texas at Austin, Austin, Texas 78758

[4]Department of Physics and Geology, University of Texas-Pan American, Edinburg, Texas 78541

Received 30 September 2008; revised 1 September 2009; accepted 7 September 2009
DOI: 10.1002/polb.21842
Published online in Wiley InterScience (www.interscience.wiley.com).

ABSTRACT: SU8 has been modified with photoinitiators Rose Bengal, H-NU 470 and H-NU 535, to conduct visible light lithography. The thermophysical properties of the lithographically transformed modified SU8 photoresins were investigated. The influence of the concentration of visible light photosensitizer and photoinitiator as well as exposure time to visible laser on thermal stability and curing kinetics were analyzed. Significant differences in the thermophysical properties were observed in these three photoinitiator groups of modified SU8 photoresins. These results provide with usable quantitative information regarding resin formulation to optimize lithography processing parameters, and therefore, the ultimate properties of lithographically formed microstructures. © 2009 Wiley Periodicals, Inc. J Polym Sci Part B: Polym Phys 48: 47–54, 2010

KEYWORDS: curing kinetics; differential scanning calorimetry (DSC); microstructure; photoinitiator; photopolymerization; SU-8; thermal stability; thermogravimetric analysis (TGA); UV-Vis spectroscopy

INTRODUCTION SU8 is an epoxy-based negative resist that was first developed by IBM in 1989.[1,2] It is sensitive to near UV radiation and has been extensively used in conventional UV photolithography. Turberfield and coworkers[3] have used SU8 for the fabrication of nanostructures/microstructures as photonic crystal templates using multi-beam interference holographic lithography with a 355 nm UV laser. Recently, Yang et al.[4] and one of the authors (Lin)[5,6] have developed a visible light holographic lithography for the fabrication of microstructures as photonic crystal templates using a modified SU8 photoresin, designed to extend the photosensitivity of commercial SU8 from UV to the visible range. The modified SU8 photoresin mixture consisted of the epoxy resin, a visible light photosensitizer, and a photoacid generator, all dissolved within a solvent. The visible light photosensitizer would absorb the radiation at a visible wavelength and form a charge transfer complex in conjunction with the photoacid generator to create the Lewis acids that would initiate ring-opening polymerization of epoxies upon heating above a critical temperature. In the case of single-photon lithography, a post-exposure baking is usually required for the polymerization to occur. If using femto-second pulses for microstructuring SU8, two-photon polymerization can occur without a post-bake due to enough local heating from the high-energy laser pulse.[7]

Despite the great advances that have been accomplished in the holographic fabrication process of microstructures using the modified SU8 photoresin with visible light sensitivity, the appearing structural shrinkages or cracks have caused serious problems to the polymeric multi-dimensional templates.[5,6,8] Volume shrinkages of up to 40% have been reported for SU8 microstructures, these shrinkages might exist due to the high volume fractions of partially crosslinked SU8.[8] It is important to mention that fabricated SU8 microstructures could be exposed to high temperature should they be intended for conversion to a high refractive index material such as silicon, with the purpose of creating complete photonic band gap materials.[9] However, their thermal stability might forbid such high temperature conversion. Thermophysical analysis of UV-sensitive SU8 has been conducted as a function of photoinitiator and exposure dose for the optimization of SU8 processing parameter.[10,11] It has been observed that by making small changes in the concentration of the chemical components, such as that of the UV photoinitiator, the results are significantly altered.[10,11] To the best of our knowledge, no thermophysical studies have been conducted on modified SU8 photoresins, sensitive to visible light. It is therefore important to understand the curing kinetics and thermal stability of the fabricated microstructures, to optimize the lithography processing parameters

Correspondence to: K. Lozano (E-mail: lozanok@utpa.edu)
Journal of Polymer Science: Part B: Polymer Physics, Vol. 48, 47–54 (2010) © 2009 Wiley Periodicals, Inc.

TABLE 1 Composition of Different SU8 Based Modified Photoresins

Samples	Contents				
	Photosensitizer	Conc. wt %	Photoacid Generator	Conc. wt %	SU8 wt %
A, A3, A4, A5	Rose Bengal	2	Diaryliodonium Hexafluoroantimonate	3	95
B, B3, B4, B5	HNU 535	0.6	Iodonium Hexafluoroantimonate (OPPI)	1.6	97.8
C, C3, C4, C5	HNU 535	2	Iodonium Hexafluoroantimonate	5	93
D, D3, D4, D5	HNU 535	0.2	Iodonium Hexafluoroantimonate	2.5	97.3
E, E3, E4, E5	HNU 470	0.1	Iodonium Hexafluoroantimonate	2.5	97.4
F, F3, F4, F5	HNU 470	0.25	Iodonium Hexafluoroantimonate	2.5	97.25

based on the modified SU8 photoresin. The objective of this study is to analyze the effect of commonly used visible light photoinitiators and photosensitizers on the degree of curing, curing rate, and thermal stability of modified SU8 photoresins designed to extend its absorption from UV to the visible range. Thermogravimetric (TGA) and Differential Scanning Calorimetry (DSC) analyses were performed on several SU8 modified resins to study their photocuring behavior. Finally, profilometry and SEM analyses were conducted to characterize the physical dimensions of the produced microstructural features.

EXPERIMENTAL

Materials

Commercially available SU8 obtained from Microchem Corporation was used to prepare six different modified photoresin mixtures. HNU 535 (Spectra Group), a photosensitizer with maximum optical absorption in the visible range at 535 nm, was used to prepare three of them. HNU 470 (Spectra Group), another visible light photosensitizer with maximum optical absorbance at 470 nm was used to prepare two more photosensitive resin mixtures. The remaining mixture was prepared with Rose Bengal (Aldrich) visible light photosensitizer. Rose Bengal has a maximum optical absorbance at 535 nm approximately. Diaryliodonium Hexafluoroantimonate (Polyset) and Iodonium Hexafluoroantimonate (OPPI) (Spectra Group) were used as photoacid generators. All the samples and their different compositions and concentrations are depicted in Table 1. The samples will be referred to as A, B, C, D, E, and F, each one having different subindices indicating their time of exposure to laser light. For example, sample A corresponds to the raw or pristine unexposed mixture, whereas A3 corresponds to the sample exposed for 3 min, A4 to 4 min, and A5 to 5 min of exposure, respectively. Samples B, C, D, E, and F follow the same nomenclature.

Microstructure Fabrication

The photosensitizer and photoacid generator were first dissolved in 10 mL of Tetrahydrofuran (THF) with the aforementioned concentrations. Later, they were stirred with a magnetic bar on a hot plate for 10 h at a stirring speed of 125 rpm. After this, the SU8 was added to the mixture and stirred again for 48 h at the same speed. For the thermophysical studies, a fairly large amount of sample (10 mg) was needed. Thus, the samples were prepared by spin-coating SU8 onto a glass substrate at spin-speed of 800 rpm to produce thick films with thicknesses of ~20 μm, which were measured by FILMETRICS. For Scanning electron micrograph (SEM) analysis, thinner films were needed, and therefore, the spin-coating speed was set between 2000 rpm and 4000 rpm. The samples were then prebaked at 65 °C for 10 min and at 95 °C for 25 min to get rid of any excess of solvent present in them. Visible light lithography was performed with a 532 nm continuous wave Compass laser (Coherent) with different exposure times of 3, 4, and 5 min at an average power of 55 mW with a power density of 142.85 W/cm^2. The lithography was examined through fabrication of one-dimensional grating structures with a two-beam interference optical setup as shown in Figure 1. The incident beam was split into two beams by an optical beam splitter. After being reflected by mirrors, these two beams overlap and form an interference pattern. After laser exposure, the samples were baked for 1 min at 65 °C and for 5 min at 95 °C to complete the polymerization reaction process. The unexposed and unpolymerized areas were washed away by developing the sample for 5 min in SU8 developer solvent (Microchem). After this step, the sample was rinsed with isopropanol and dried.

UV-Vis Spectroscopy

The absorption spectra of the modified SU8-based photoresins were recorded with a DU 800 Spectrometer (Beckman-Coulter) in a wavelength range varying from 300 nm to 700 nm.

Differential Scanning Calorimetry

The thermal calorimetric properties of the resins were studied using a TA Instruments Differential Scanning Calorimetry (DSC) Q100 device. The samples were heated from 40 °C to 250 °C at a rate of 5 °C/min, cooled down from 250 °C to 40 °C at the same rate, heated up from 40 °C to 250 °C and cooled down again from 250 °C to 40 °C at the same rate. These heating and cooling cycles were performed in aluminum hermetic pans under nitrogen atmosphere with a flow rate of 50 mL/min.

Thermogravimetric Analysis

Thermal stability and weight loss studies were performed on a TA Instruments Thermogravimetric Analysis (TGA) Q500 device. The samples were analyzed from 20 °C to 1000 °C at a heating rate of 10 °C/min. All the analyses were performed under nitrogen atmosphere with a flow rate of 40 mL/min.

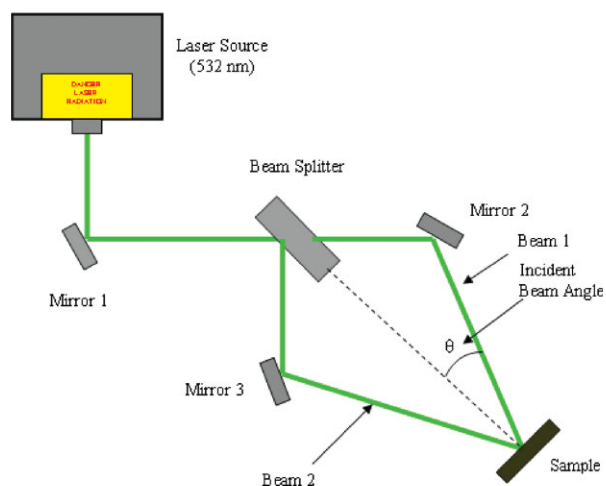

FIGURE 1 Optical setup for holographic fabrication of micro-gratings. [Color figure can be viewed in the online issue, which is available at www.interscience.wiley.com.]

Scanning Electron Microscopy

An Emitech sputter system was used to deposit a thin film of silver (~10 nm) on the specimens before analysis on a Zeiss Neon 40 field emission-scanning electron microscope (FE-SEM) working under acceleration voltages of 5 keV. The secondary electron detector was used to acquire the SEM images.

Profilometry Analysis

A Veeco Dektak 150 profilometer instrument was used to characterize the dimensions of grating period and grating height of the produced SU8 modified photoresin microstructure. The Dektak tool has a wide range of measurements (>6 mm), and this makes possible to perform auto-leveling of the sizes according to unpatterned locations and provides absolute amount of displacement. A millimeter-range surface map was used to illustrate the uniformity and periodicity of our fabricated microstructures.

RESULTS AND DISCUSSION

Figure 2 shows the UV-Vis spectra graph of the modified photoresins and pristine SU8 for comparison. Samples A and C have strong absorption in the visible range. Sample D has the smallest concentration of photosensitizer and photoinitiator, thus, it shows a weak peak with value of 1 at 500 nm. It reaches the highest value below 400 nm, where its SU8 component has stronger absorption. Pristine SU8 shows negligible absorption from 800 to 365 nm. Right at 365 nm it starts to show sudden and strong absorption values as expected, given its natural strong absorption in the UV range. Sample E shows weak absorption around 470 nm due to a scarce concentration of photoinitiator. Sample F on the other hand shows its highest absorption values for the visible range approximately at 470 nm as expected, since its photosensitizer concentration is higher than in sample E.

As mentioned before, SU8 modified microstructures created by visible light lithography (or other methods) could have a significant number of potential applications. Therefore, it is important to analyze its thermophysical stability in a wide temperature range. Figure 3(a) shows the DSC scans for sample A, A3, A4, and A5. A large exothermic peak at 150 °C is observed for A in the first heating cycle and disappears in the second heating cycle. This peak was also observed by Lian et al. who concluded that this particular peak is strongly related to the addition of the UV photoinitiator.[10] This peak represents the crosslinking reaction occurring during the heating scan. The area under the curve of this peak is ΔH or the change in enthalpy necessary for the resin to undergo a curing reaction. In the second heating cycle, ideally, there should be no peak indicating that all the material has already been cured or crosslinked and will not undergo further structural transformation. As a matter of fact, no peak should be observed even in the first heating cycle which would signify that the lithography process was efficient and the material is ready to be used. This exothermal peak has a value of $\Delta H = 104.2$ J/g. It can be observed that the exposed samples still show an exothermic reaction (though with different enthalpies) independently of the exposure time. The ΔH value for sample A5 which has the smallest value is 50.25 J/g (Table 2 lists ΔH values for all samples). This value even though smaller, still represents a large exothermic reaction, and therefore, microstructural changes within the sample will occur at this temperature which is the temperature at which most IC components operate.

B samples have similar behavior to A samples and the scans are shown in Figure 3(b). Their exothermic peaks start again at 150 °C with the unexposed sample having the greatest peak with $\Delta H = 295.8$ J/g. Figure 3(c) shows the DSC scans for C samples. These samples have the greatest concentration of photoinitiator. A clear difference with all other samples is observed. The large exothermic peak is seen for the unexposed sample, though in this case the peak now disappears for the exposed samples. It is evident that the

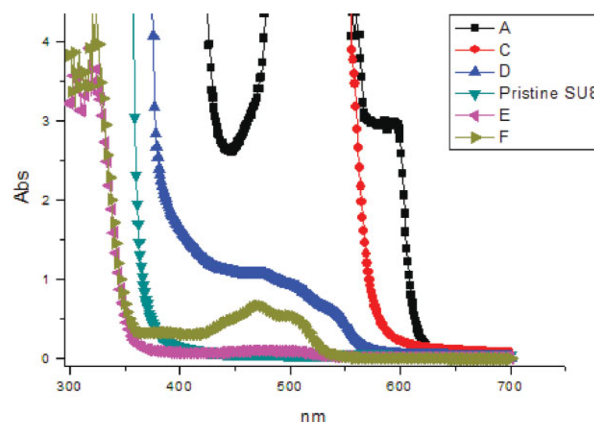

FIGURE 2 UV-Vis absorption spectra for samples A, C, D, E, F and pristine SU8. [Color figure can be viewed in the online issue, which is available at www.interscience.wiley.com.]

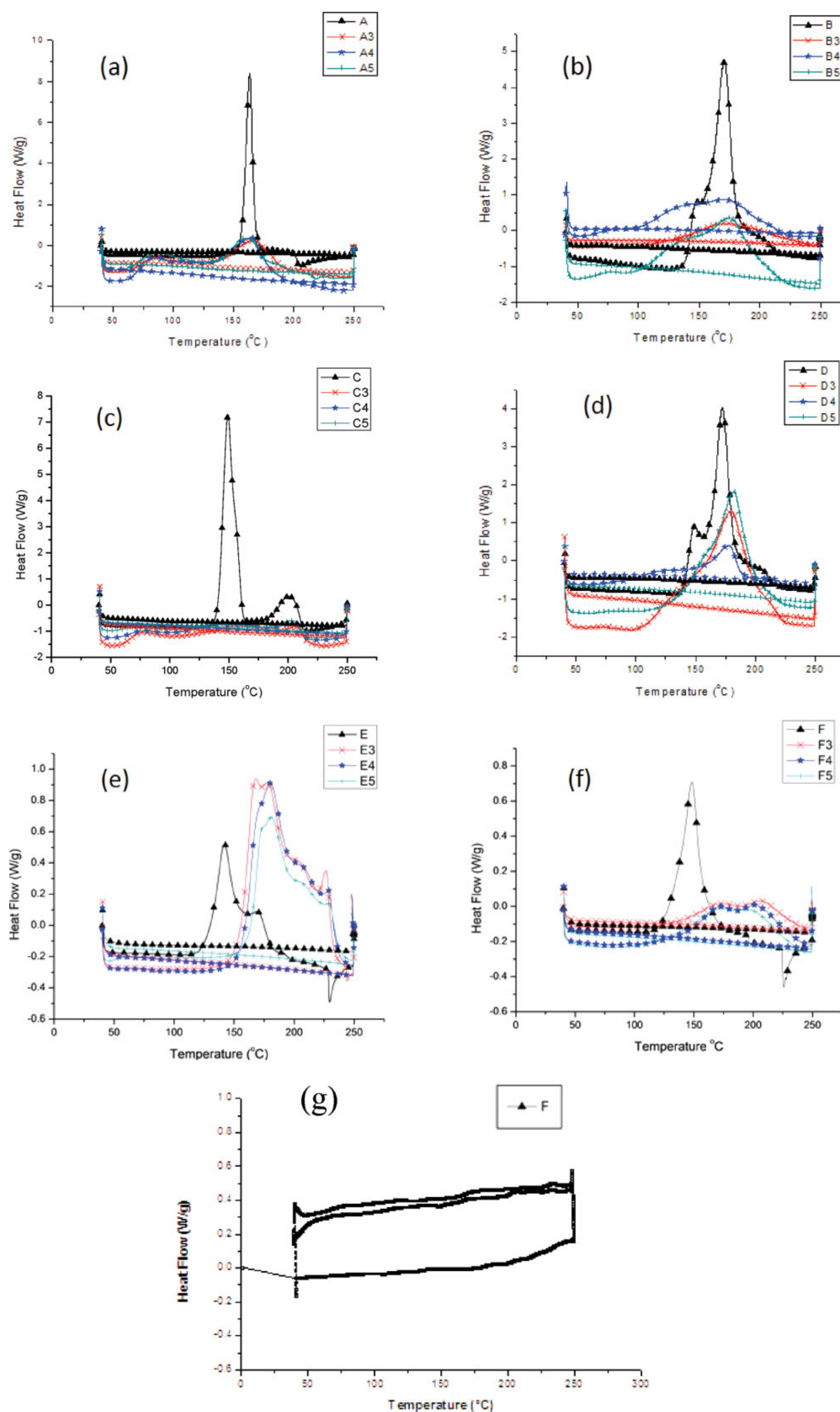

FIGURE 3 DSC scans for different exposure times. (a) DSC scans of A samples for different exposure times, (b) DSC graph of B samples for different exposure times, (c) DSC scans of C samples for different exposure times, (d) DSC scans of D samples for different exposure times, (e) DSC scans of E samples for different exposure times, (f) DSC scans of F samples for different exposure times, and (g) DSC scan of F sample with two-step further laser treatment. [Color figure can be viewed in the online issue, which is available at www.interscience.wiley.com.]

TABLE 2 Δ*H* (Enthalpy Difference) Values of the Different Mixtures Measured by DSC

	Δ*H* (J/g)		Δ*H* (J/g)
Sample A		Sample B	
A	104.2	B	295.8
A3	74.48	B3	204.7
A4	55.61	B4	182.6
A5	50.25	B5	179.3
Sample C		Sample D	
C	286.09	D	244.5
C3	12.59	D3	191.5
C4	10.51	D4	190.1
C5	9.772	D5	187.1
Sample E		Sample F	
E	265.9	F	241.6
E3	790.9	F3	132.5
E4	680.1	F4	197.9
E5	489.1	F5	223.2

concentration of photoinitiator strongly affects crosslink density and curing rate.

Figure 3(d) shows the DSC scans for D samples. These samples have the least concentration of photoinitiator and this fact is shown by the great values of ΔH for the irradiated samples. The ΔH values for these irradiated samples range from 244.5 J/g for D to 187.1 J/g for D5 in comparison with 9.7 J/g for C5. This is the contrasting evidence of the lack of effectiveness of the crosslinking mechanism due to insufficient photoinitiator concentration. Table 2 summarizes the values of ΔH for the different mixtures.

Figure 3(e) shows the DSC scans for E samples. These have the highest ΔH values of all the analyzed samples, ranging from 265.9 J/g to 790.9 J/g. Their low concentration of photonitiator and the use of photosensitizer with maximum absorbance at 470 nm were the responsible factors for the sample not obtaining sufficient radiation energy, and thus, presenting deficient curing.

Figure 3(f) shows the DSC scans for F samples. These samples show similar enthalpy values when compared to D samples. This can be seen and explained by the similarities in their absorption profiles (Fig. 2). F samples have a slightly higher photosensitizer concentration than D samples, which is counterbalanced by the fact that it comes from a 470 nm absorbing photosensitizer.

According to Lian et al., the percentage of mass loss of SU8 materials depends on the irradiation doses administered to them.[10] Figure 4(a) shows the TGA curves for unexposed and exposed A samples. It is observed that the unexposed sample suffers from 25% mass loss starting at 100 °C. Exposed samples A3, A4, and A5 show a considerable increase in thermal stability by the pinning of the molecules through the crosslinking mechanism that has occurred in them. No clear difference is observed among A3, A4, and A5. Samples B and C behave similar to Sample A. However, Sample D, having the least concentration of photoinitiator shows greater mass loss and a clear distinction with exposed samples. D3 is showing greater mass loss when compared to D4 and D5. Figure 4(b) shows the TGA curves for D samples.

E samples have similar behavior to D samples. There is a marked difference between the thermal stability of the unexposed and exposed samples because of the pinning reinforcing mechanism on the polymer chains [Fig. 4(c)]. F samples look similar to E samples featuring higher percentages of massloss values due to a lower photosensitizer concentration [Fig. 4(d)].

SEM analysis was conducted to check lithography formed microstructures on each group of the samples. Figure 5(a) shows SEM of microstructures formed in Rose Bengal modified SU8 photoresin. The sample was prepared with spin-coating speed of 4000 rpm (thickness ~ 9 microns as measured by FILMETRICS) with an exposure time of 3 min. It clearly shows 1D grating formed through visible light lithography. Figure 5(b) shows SEM of microstructures formed in H-NU535 modified SU8 sample C3. The exposure time is also 3 min but overexposure was observed when compared to Figure 5(a). It is reasonable, given the fact that H-NU 535 had been reported to have higher quantum yield to donate electrons than Rose Bengal.[4] When reducing the exposure time to 1 min, a much clear groove was formed in 1D grating as shown in Figure 5(c) in a sample prepared with a spin-coating speed of 3000 rpm. For H-NU 470 modified SU8 photoresin, the grating formed through 532 nm lithography always shrank due to the fact that the absorption of H-NU 470 is very low at 532 nm as seen in Figure 2. Under the exposure of 488 nm Ar-ion laser, a clear structure was formed in the H-NU 470 modified SU8 photoresin as shown in Figure 5(d). This sample was prepared with a spin-coating speed of 2000 rpm. The Ar-ion laser power was 413 mW with a power density of 1147 mW/cm^2. The exposure time was 20 s. From Figure 5, it is evident that visible light lithography had been achieved in all three photoinitiator groups of modified SU8 photoresin.

Profilometry analysis was performed to characterize its physical dimensions such as period and grating height. In this manner, results obtained from SEM analysis on microstructure morphology can be further confirmed. Figure 6(a) shows results conducted on HNU-470 modified SU8 photoresin sample, grating height results appear as periodic gradients both in the plane and 3D space, thus denoting the periodic nature of the microstructure over a larger area. This sample was prepared with a spin-coating speed of 2000 rpm. The Ar-ion laser power was 660 mW with a power density of 1833 mW/cm^2. The exposure time was 20 s. Figure 6(b) shows the period between two peaks that correspond to two gratings and is equal to 2.43 μm as can be seen also from Figure 5(a,b). Figure 6(c) shows a similar graph that presents the approximate grating height of the microstructure. It has a value of 1.08 μm. It is noteworthy to

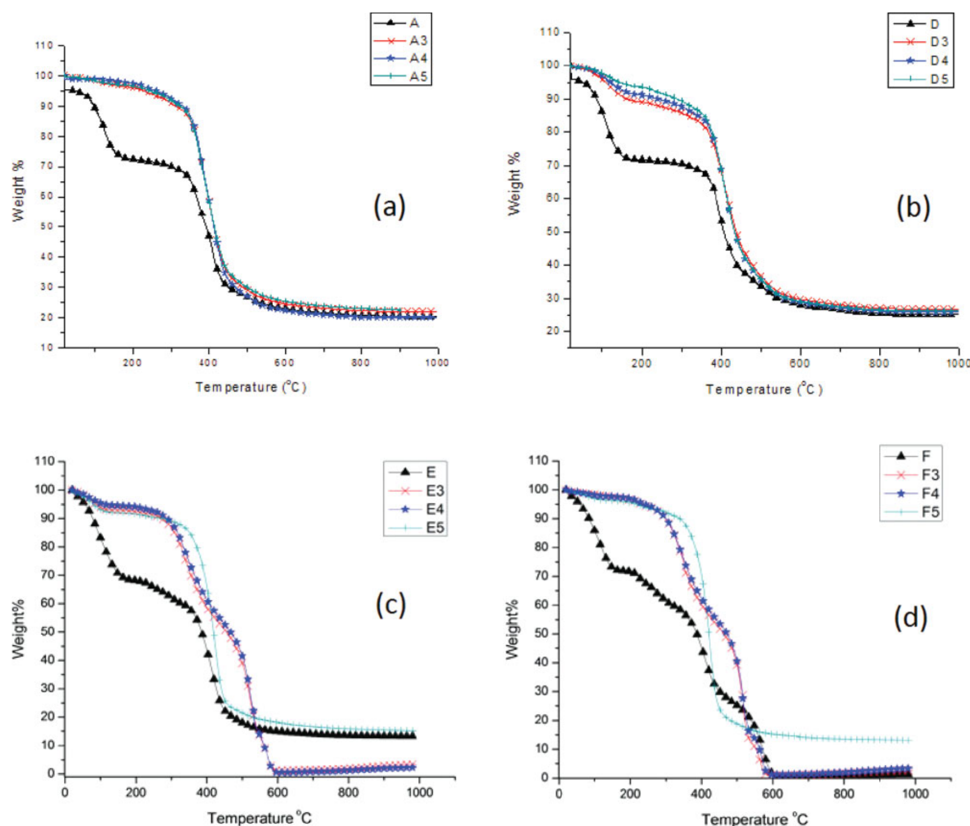

FIGURE 4 TGA curves for different exposure times. (a) TGA curves of A samples for different exposure times, (b) TGA curves of D samples for different exposure times, (c) TGA curves of E samples for different exposure times, and (d) TGA curves of F samples for different exposure times. [Color figure can be viewed in the online issue, which is available at www.interscience.wiley.com.]

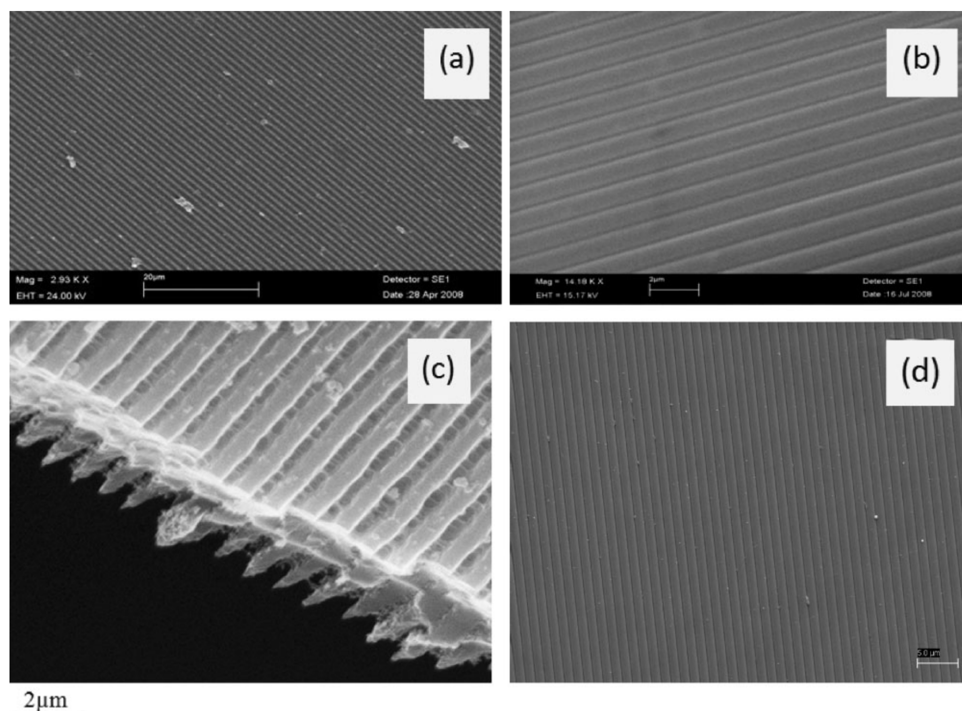

FIGURE 5 SEM results. (a) Rose Bengal modified SU8 photoresin microstructure, (b) HNU 535 modified SU8 photoresin microstructure, (c) Cross sectional SEM of HNU 535 modified SU8 microstructure, and (d) HNU 470 modified SU8 photoresin microstructure.

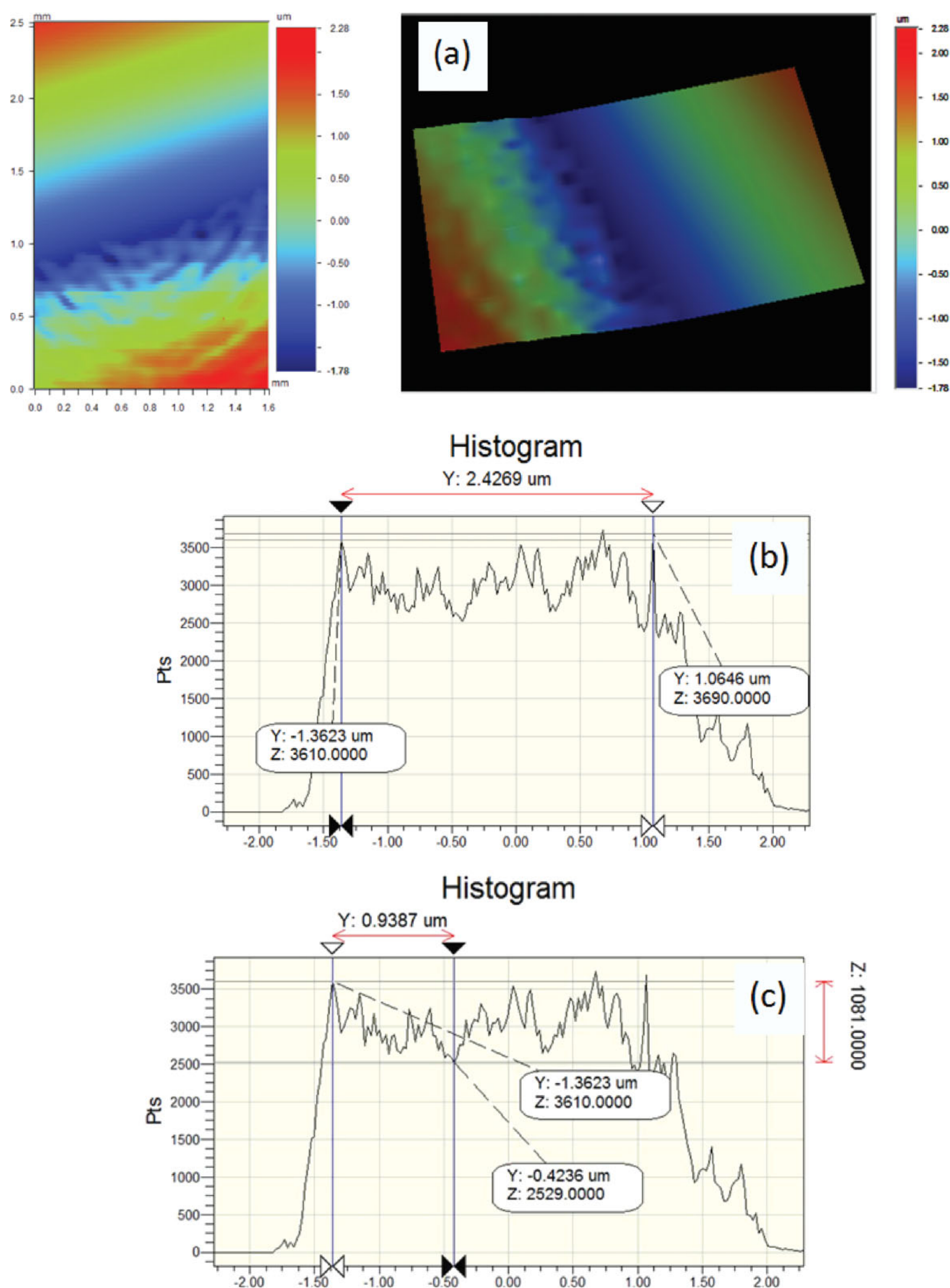

FIGURE 6 Profilometry results. (a) Profilometry images, surface and 3D space, (b) Histogram of the period of the sample, and (c) Histogram of the height of the sample.

remark that this value of grating height is the result after the polymerization process and it differs from the thickness results obtained for samples taken after the spin-coating process.

From the above studies, we can relate absorption and thermophysical studies to the lithography processing. If the absorption to the laser beam is low in the modified SU8 due to the concentration of photoinitiators or the absorption property of

individual photoinitiator, less photoacid is generated with same exposure time for polymerization in the post-exposure baking. Thus, the enthalpy difference is high in the lithographic microstructure and the thermal stability is poor due to low volume fraction of polymerization in the structure. Long exposure time can improve the thermal stability, however, over-exposure can occur as seen from SEMs. From these studies, it is suggested that two-step process can be developed to improve the lithography and thermal stability of the lithographic microstructure. First step, microstructures are formed through the lithography with a less but desired exposure time. Then, the developed lithographic microstructures receive further uniform laser exposure to further improve the thermal stability. A microstructured HNU-470 modified SU8 photoresin sample was prepared using Ar-ion laser 488 nm beam with a power density of 3888 mW/cm^2 and an exposure time of 3 s. After post-bake, development, and drying, the sample received a further exposure under an expanded uniform beam with a power density of 3710 mW/cm^2 for 135 s. After post-bake, DSC analysis was performed on the sample and the result is shown in Figure 3(g). The DSC test shows that the sample was completely cured as there are two flat lines and no exothermic reactions.

CONCLUSIONS

A study was performed to analyze the effect of commonly used visible light photoinitiators and photosensitizers, their concentration and exposure to laser radiation on the curing behavior and thermal stability of produced SU8 modified photoresins. It is important to understand curing kinetics and thermal stability of these modified SU8 photoresin materials given the wide range of temperatures at which they can be subjected. Complete curing is essential for several engineering applications. Partially cured epoxies could be severely affected by temperature, and significant microstructural changes could occur in them, leading to failure of the part in a working environment. DSC and TGA analysis showed clear differences as a function of exposure times and photoinitator concentration. It was observed that C samples showed an optimal concentration and no further microstructural changes are expected to occur in them. Mixtures B, D, E, and F have lower concentrations of photoinitiator, and therefore, showed a poor thermal stability. Large exothermal peaks were observed indicating that the samples will undergo microstructural changes when exposed to temperatures above 150 °C. SEM analysis was conducted to observe the morphology of the lithographic microstructures and the results were related to their respective degrees of photopolymerization. Profilometry analysis was finally conducted to characterize the period and grating height of modified SU8 photoresin microstructures. The results showed that the periodicity of the sample extends over a large area and that the period value of the sample matches those results previously stated by SEM analysis.

The authors thank the Biology Department at UTPA, especially Anxiu Kuang, for her SEM support. The authors acknowledge financial support from National Science Foundation under the award of CMMI-0609345.

REFERENCES AND NOTES

1 Gelorme, J. D.; Cox, R. J.; Gutierrez, S. A. R. (IBM Co.). U.S. Patent 4,882,245, November 21, 1989.

2 Shaw, J. M.; Gelorme, J. D.; Labianca, N. C.; Conley, W. E.; Holmes, S. J. IBM J Res Dev 1998, 41, 81–94.

3 Campbell, M.; Sharp, D. N.; Harrison, M. T.; Denning, R. G.; Turberfield, A. J. Nature 2000, 404, 53–56.

4 Yang, S.; Megens, M.; Aizenberg, J.; Wiltzius, P.; Chaikin, P. M.; Russel, W. B. Chem Mater 2002, 14, 2831–2833.

5 Lin, Y.; Herman, P. R.; Darmawikarta, K. Appl Phys Lett 2005, 86, 071117, 1–3.

6 Poole, Z.; Xu, D.; Chen, K. P.; Olvera, I.; Ohlinger, K.; Lin, Y. Appl Phys Lett 2007, 91, 251101, 1–3.

7 Seet, K. K.; Juodkazis, S.; Jarutis, V.; Misawa, H. Appl Phys Lett 2006, 89, 024106.

8 Meisel, D. C.; Diem, M.; Deubel, M.; Perez-Willard, F.; Linden, S.; Gerthsen, D.; Busch, K.; Wegener, M. Adv Mater 2006, 18, 2964–2968.

9 Tétreault, N.; Freymann, G.; Deubel, M.; Hermatschweiler, M.; Pérez-Willard, F.; John, S.; Wegener, M.; Ozin, G. A. Adv Mater 2006, 18, 457–460.

10 Lian, K.; Ling, Z. G.; Liu, C. Proceedings of SPIE 2003, 4980, 208–212.

11 Lorenz, H.; Despont, M.; Fahrni, N.; Labianca, N. Sens Actuators A 1998, 64, 33–39.